Desalination and Water Treatment
www.deswater.com
doi: 10.1080/19443994.2015.1067166

57 (2016) 14552–14564
July

Taylor & Francis
Taylor & Francis Group

Sorption performance of lithium-doped titanium vanadate for Sr^{2+}, Fe^{3+} and Al^{3+} from polluted water

Ismail M. Ali[a], Mohammed A. Gomaa[b], Ibrahim M. El Naggar[a], Jilan A. Omar[b,*], Mohammed F. El-Shahat[c]

[a]*Hot Lab. Center, Atomic Energy Authority, Cairo, Egypt, Tel. +2/01119620025; email: ismail_m_ali@yahoo.com (I.M. Ali), Tel. +2/01008077210; email: El-naggar@yahoo.com (I.M. El Naggar)*
[b]*Hydrogeochemistry Department, Desert Research Center, Al-Matariya, Cairo, Egypt, Tel. +2/01002071713; email: gomaa_57@yahoo.com (M.A. Gomaa), Tel. +2/01141782856; email: dr_gilanomar@hotmail.com (J.A. Omar)*
[c]*Faculty of science, Chemistry Department, Ain Shams University, Cairo, Egypt, Tel. +2/01128323115; email: elshahatmf@hotmail.com*

Received 19 November 2014; Accepted 10 June 2015

ABSTRACT

Lithium-doped semicrystalline titanium vanadate (TV) with enhanced sorption properties was obtained using one step precipitation method. Employing this technique at different precipitation conditions produced two lithium-modified forms (LTVI and LTVII). The materials were characterized by X-ray diffraction (XRD), infrared spectroscopy (IR), simultaneous thermal analysis (DTA/TGA), and scanning electron microscopy (SEM). Stability of the materials was investigated. The XRD patterns of different vanadate forms revealed poor crystalline nature with minor changes. Distribution coefficient (K_d) of Sr^{2+}, Fe^{3+}, and Al^{3+} on different vanadate forms was studied and it was found that the selectivity order is $Sr^{2+} > Fe^{3+} > Al^{3+}$. In addition, it can be seen that LTVI (of higher Li^+ content) shows the higher sorption efficiency, mechanical, and chemical stability compared to the other forms. The dependence of sorption capacity of LTVI on annealing temperature was also studied. The study of binary separation of metal ions showed that LTVI can be potentially useful for analytical applications. Thermodynamic parameters of the exchange process employing the Van't Hoff equation announced that the exchange reactions are endothermic and spontaneous. Langmuir and Freundlich isotherm models were applied to the experimental data to examine the exchange mechanism.

Keywords: Lithium-doped titanium vanadate; Equilibrium studies; Selectivity; Thermodynamic

1. Introduction

In recent years, synthetic inorganic ion exchangers have gained much attention owing to their high selectivity for certain elements, better kinetics of exchange and besides other advantages, are more stable at high temperatures and in radiation fields than the organic ion exchanger [1–5]. Most investigations have been concerned with the use of these materials in the separation and removal of heavy toxic metal ions. These toxic metals are generated as untreated or partially treated

*Corresponding author.

by-products of various industries and due to unsafe storage of hazardous radioactive elements [6,7]. The toxic metal ions when present in water are injurious to health. Hence, it is very important to treat such water to remove these hazardous ions before it is supplied for any useful purpose [8]. Synthesis of novel ion exchangers are always of interest since they are selective in nature compared to commercial resins which show high capacity, but poor selectivity toward different metal ions [9]. Among these synthesized crystalline or amorphous materials, dual inorganic ion exchangers (polyoxometalates) were found to show relatively increased ion exchange capacity and selectivity in comparison to others. Various types of these useful compounds have been synthesized until now [10,11]. These materials are usually acid salts of multivalent metals. These inorganic ion exchangers were found to show relatively increased ion exchange capacity and selectivity and played a prominent role in water processing in the chemical and nuclear industries [12,13].

Recently, separation of some hazardous cations using titanium vanadate has been reported [14]. Among the methods applied to enhance the selectivity and capacity of adsorbent materials is the enriching of the material matrix with ions of small ionic radii. Accordingly, Li^+ *in situ* doping is one among the tools applied to develop the sorption performance. In this concern, ultra-fine powder $Li_4Mn_5O_{12}$ was prepared and used as selective sorbent for Li^+ [15]. In 2013, H_2TiO_3 was obtained from the acid-modified adsorbent precursor Li_2TiO_3, which was synthesized by a solid-phase reaction between TiO_2 and Li_2CO_3 [16]. This modified material was applied to extract lithium ion from LiCl solution in the presence of magnesium ions. Therefore, more attention has been given toward increasing the sorption efficiency of titanium vanadate.

In the present work, attempts have been made to obtain a new heterogeneous ion exchanger-based titanium vanadate (TV) by doping TV with lithium ions. Synthesis, characterization, metal ion removal characteristics, and analytical application of material were reported.

2. Materials and methods

All reagents and chemicals utilized in this work were of analytical grade purity, and purchased from Sigma-Aldrich.

2.1. Preparation of titanium vanadate and lithium modified titanium vanadates

Titanium vanadate (TV) was prepared in laboratory by dropwise addition of equal volumes of 0.5 M $TiCl_4$ (dissolved in 2 M HCl, MW = 189.68, purity ≥ 99%) and 0.5 M $NaVO_3$ (MW = 121.93, purity ≥ 98%, Sigma-Aldrich) (pH 11) with constant stirring. Lithium titanium vanadate I (LTVI) was prepared in laboratory by dropwise addition of equal volumes of 0.25 M LiCl (MW = 42.39, purity ≥ 99.99%), 0.5 M $TiCl_4$ (dissolved in 2 M HCl), and 0.5 M $NaVO_3$ (pH 11) with constant stirring. Ammonia solution was used as precipitating agent in each previous reaction. Lithium titanium vanadate II (LTVII) was prepared by dropwise addition of 0.5 M $LiOH{\cdot}H_2O$ (MW = 41.96, purity ≥ 99.995%) to a mixture of equal volumes of 0.5 M $TiCl_4$ and 0.5 M $NaVO_3$ with constant stirring. After an overnight standing in mother liquor, the obtained yellow precipitates were filtered, washed thoroughly with bidistilled water then dried in an air oven at 60 ± 1°C. The produced materials were rewashed with bidistilled water in order to remove any fine adherent particles and finally air dried to appear in dark brown shiny particles.

2.2. Characterization of materials

Sorption properties of the obtained materials can be evaluated according to physicochemical properties. Apparent investigations indicated that, LTVI is more physically suitable than TV and LTVII.

2.3. X-ray diffraction, SEM, IR spectra and DT/TGA thermal analysis

Powder X-ray diffraction (XRD) patterns were carried out using Shimadzu X-ray diffractometer, Model XD 490 Shimadzu, Japan, with a nickel filter and Cu–Kα radiation tube. The scanning electron microscopy (SEM) photographs were carried out for three samples. Using SEM Model Philips XL 30 attached with EDAX Unit, with accelerating voltage 30 kV, magnification 10× up to 400,000×. Samples are coated with gold. The Fourier transform infrared spectra were measured with BOMEM FT-IR spectrometer; MB 147, Canada on KBr disk technique in the range 400–4,000 cm^{-1}. Thermal stabilities, water contents and the solid state dehydration changes of the obtained materials were carried out using a DT-60H thermal analyzer, Shimadzu, Japan. The sample measured from ambient temperature up to 1,000°C with a heating rate of 15 deg min^{-1} in nitrogen gas atmosphere.

2.4. Elemental analysis

Elemental composition of the differently prepared vanadates was performed by X-ray fluorescence (XRF) of solid samples with Philips XRF detector, PW-1200

Table 1
Elemental analysis and the expected formula of the prepared exchangers

Exchanger	TiO_2%	V_2O_5%	Li_2O%	H_2O%	Expected empirical formula
TV	36.56	45.2	–	17.6	$(TiO_2)_{1.8}$ (V_2O_5) $(H_2O)_{3.90}$
LTVI	35.70	45.2	2.42	16.7	$(TiO_2)_{1.75}$ (V_2O_5) $(Li_2O)_{0.25}$ $(H_2O)_{3.75}$
LTVII	41.25	41.0	1.33	16.4	$(TiO_2)_{2.3}$ (V_2O_5) $(Li_2O)_{0.15}$ $(H_2O)_{4.0}$

sequential spectrometer, Holland. Lithium content was determined using Jenway Flame photometer PfP7. The chemical data of the products are given in (Table 1).

2.5. Chemical stability

About 0.5 g of each TV, LTVI, and LTVII was equilibrated with 50 ml solutions of analytical interest at room temperature (25 ± 1˚C) and kept for 24 h with intermittent shaking. The percent of weight loss was determined and shown in (Table 2).

2.6. Equilibrium studies

2.6.1. Distribution studies

The distribution coefficient (K_d) is an experimental way of determining the affinity of sorbent material for a specific ion. The K_d values for the studied metal ions were determined using batch experiments by shaking 0.1 g of TV, LTVI, and LTVII samples with 10 ml of 100 ppm of Sr^{2+}, Fe^{3+}, and Al^{3+} at 25 ± 1˚C. The initial pH of the solution was adjusted to pH 1–5 with 0.1 mol/dm^3 HNO_3. After equilibrium (6 h sufficient to attain equilibrium), mixtures were centrifuged and the ion concentrations were determined using ICPseq-7500 spectrometer. The K_d values were calculated by the following relation:

$$K_d = \frac{I - F}{F} \times \frac{V}{m} \text{ ml/g} \quad (1)$$

where, I and F are the initial and final concentrations of the considered element in solution phase. V/m is the solution volume to adsorbent mass ratio (batch factor, 100 ml/g).

2.6.2. Sorption capacity

Sorption capacity (meq/g) of TV, LTVI, and LTVII was determined by batch experiment technique (Table 3) where, 0.1 g of the solid samples were equilibrated with 10-ml of 0.05 M solutions of $SrCl_2$, $Fe(NO_3)_3$ and $Al(NO_3)_3$ representing the selected metal ions (Sr^{2+}, Fe^{3+}, and Al^{3+}). After equilibration at 25 ± 1˚C, the liquid phase was separated by centrifugation and replaced by the same volume of the initial solution. The procedures were repeated until no further sorption of cations occurred. The capacity was calculated as the following:

$$\text{Capacity}\left(\frac{\text{meq}}{\text{g}}\right) = \%\text{uptake} \times C_o \times \frac{V}{m} \times \frac{Z}{100} \quad (2)$$

where Z is the charge of the considered ion and C_o is the initial concentration of the metal ion adsorbed. All the experiments were conducted in triplicate and

Table 3
Sorption capacities (meq/g) for TV, LTVI, and LTVII of Fe^{2+}, Al^{3+}, and Sr^{2+}

	Al^{3+}	Fe^{2+}	Sr^{2+}
TV	0.6	0.82	0.91
LTVI	0.73	0.95	1.16
LTVII	0.4	0.58	0.7

Table 2
Chemical stabilities (weight loss %) of the prepared exchangers in water, acid, and NaOH, V/m (ml/g) = 100, T = 25˚C and 24 h contact

Exchanger	H_2O	0.1 M HCl	0.5 M HCl	0.1 M HNO_3	0.5 M HNO_3	0.1 M NaOH
TV	0	0.5	1.4	2	1.6	4
LTVI	0	2.0	5.7	3	5.4	2
LTVII	0	4.0	9.4	5	8.0	5

average values were used in the data analysis and the results agreed to ±3%.

3. Results and discussion

TV and its modified forms (LTVI and LTVII) were prepared through one step precipitation process. Among them, LTVI (possessed better physical, mechanical, and Sr^{2+} sorption capacity) was chosen for detailed studies and characterization).

3.1. Physical characterization of the synthesized ion exchangers

Elemental analysis of TV, LTVI, and LTVII is shown in Table 1. Although the obtained TV material was modified with lithium ions, it is obvious that both TiO_2 and V_2O_5 are the main matrix components. Also all forms reveal a shiny dark brown. When Li_2O enters it decrease somewhat the percentage of TiO_2 and water content in LTVI. In contrast in LTVII, the percentage of V_2O_5 is decreased and TiO_2 is increased by doping with Li^+. At the same time, the percentage of Li_2O in LTVI is about twice its value in LTVII. Differences in elemental ratios besides the changes in mechanical properties may affect the sorption behavior of the materials.

Chemical stability of the materials was investigated in water, nitric, hydrochloric acid, and sodium hydroxide. vanadates show reasonable chemical stability in water and at low acid concentration, while they are partially dissolve in the range of 1 M either in acid or alkaline solution. The Li^+-doped forms (LTVI) showed comparable stability with un-doped one (TV).

Fig. 1(a–c) displays the DTA-TG thermograms of TV, LTVI, and LTVII samples, respectively. The Fig. 1(a–c) shows an endothermic peak with maxima at $T_m \sim 99.5$, 93.5 and 106°C for TV, LTVI, and LTVII, respectively. These peaks were almost assigned to the dehydration reactions [17,18]. The second endothermic peak appears at $T_m \sim 460$, 479, and 424°C for TV, LTVI, and LTVII, respectively. This peak was possibly due to the loss of constitution water which forms part of the crystalline network and it is generally presented like hydroxyl groups [19,20]. The total percent of mass loss for TV, LTVI, and LTVII are equal 17.3, 16.5, and 16.6%, respectively. These values represent the total water contents of materials. Accordingly, the obtained materials may be looked as Ti–V mixed hydrous oxides, which is a common behavior for many inorganic adsorbents [1,2,17]. Additionally, for the LTVI and LTVII (Fig. 1(b) and (c)), it was observed that an endothermic peak at 603 and 597°C, respectively. These peaks appear with no mass change, which may

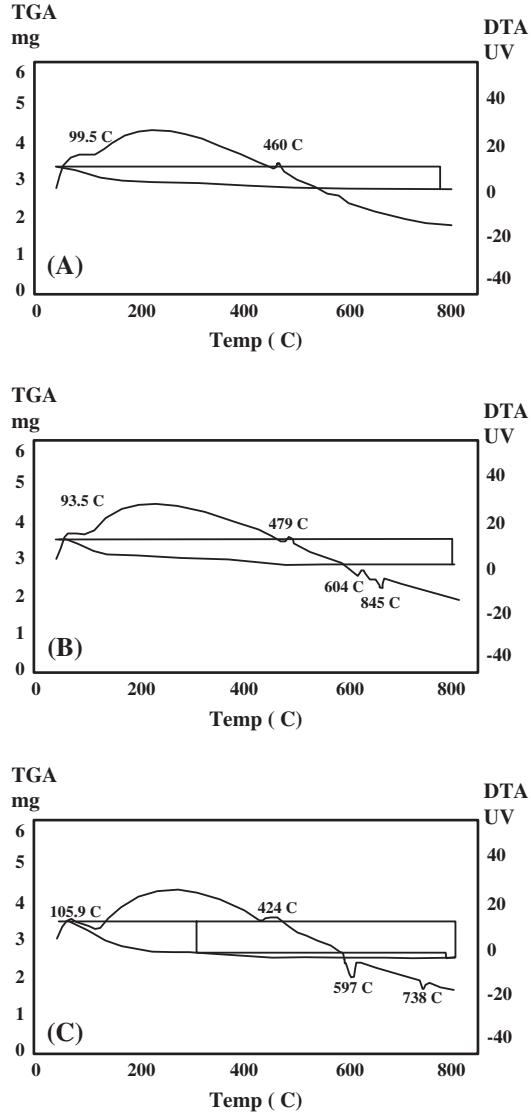

Fig. 1. DT/TGA thermograms of (A) TV, (B) LTVI, and (C) LTVII.

be attributed to an improvement in crystallinity [17,21]. Finally, an endothermic peak was observed from Fig. 1(b) and (c) at 645 and 738.7°C, respectively, which may be assigned to the oxides formation [22]. The lower percent of water content of each LTVI and LTVII than TV may be due to the substitution of Li^+ with some sites of water molecules. It can be presumed that all studied vanadates are thermally stable and have OH groups, which are important and favorable for adsrption applications.

The infrared spectra of different vanadate samples are nearly the same, just with slight differences in details. This may be due to the difference in the preparation conditions and/or surface structural

differences. Fig. 2 shows the FT-IR spectra for TV and LTV (I and II). In all spectra, the band around 3,430 cm^{-1} due to stretching mode of free water [23] and O–H group with the band at 1,626 cm^{-1} may be attributed to deformation vibration of free water [21,24]. The band at 986, 982, and 985 cm^{-1} in TV, LTVI, and LTVII, respectively may be due to the presence of vanadate ions [8,21]. From other point of view, semiquantitative IR spectra of LTVI dried at 60, 200, 400, 600, and 800˚C (Fig. 3) revealed that the main characteristic bands of vibration of water molecules (3,430, 1,626 cm^{-1}) were decreased with increasing temperature. Also, for LTVI the band at 986 cm^{-1} was shifted higher to 1,016, 1,017, and 1,016 cm^{-1} after heating at 400, 600, and 800˚C, respectively. This shift may be due the presence of multiple vanadium ions such as (V^{4+} and V^{5+}) results from lithium incorporationin in parallel with the presence of the shortest V=O bond (1.58 Å) of the vanadium pentoxide [25]. The band observed at 423 and 424 cm^{-1} for LTVI heated at 400 and 600˚C, respectively, is due to Li_2O [26]. The band at 537, 535, and 534 cm^{-1} in TV, LTVI, and LTVII spectrum, respectively, may be due to metal–oxide bonds [6,22,27]. The powder XRD patterns for the prepared TV, LTVI, and LTVII (Fig. 4) revealed that; TV has two peaks at $2\theta = 25.3^{\circ}$ and 52.3˚, LTVI record only one peak at $2\theta = 25^{\circ}$ and LTVII records three small peaks at $2\theta = 25.3^{\circ}$, 29.1˚, and 49.4˚. It can be obvious that all samples show low degree of crystallinity with slight changes. These changes may be attribted to the presence of Li ions or due to the differences in experimental conditions. On the other hand, the XRD patterns of LTVI calcined at different temperatures were studied and data are showen in Fig. 5. XRD patterns revealed that LTVI change to new phases with the increasing temprature. At 200˚C; four peaks are recorded at 400˚C; 15 peaks are recorded with crystal size range from 6.2 to 72.7 nm, at 600˚C; 17 peaks are recorded with crystal size range from 39.1 to 261.7 nm and at 800˚C; 15 peaks are recorded with crystal size range from 59.3 to 244.9 nm. The new crystalline phases obtained by heating can be attributd to the dehydration of water molecules with transformation into well crystallized oxides at high temperature [26,28,29].

The mean crystallite size (D) of LTVI in different phases was calculated by the Scherer's equation and given in (Table 4):

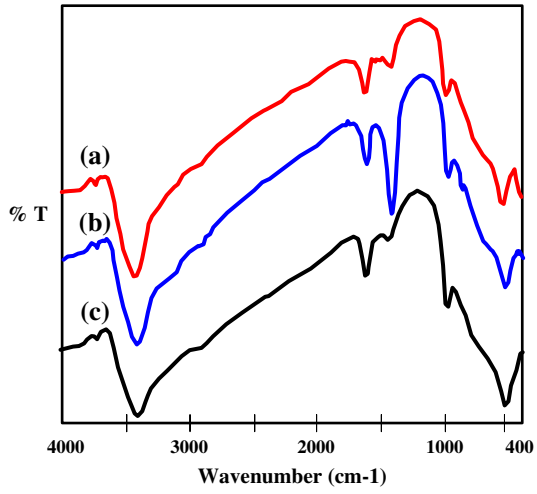

Fig. 2. IR spectra of (a) TV, (b) LTVI, and (c) LTVII.

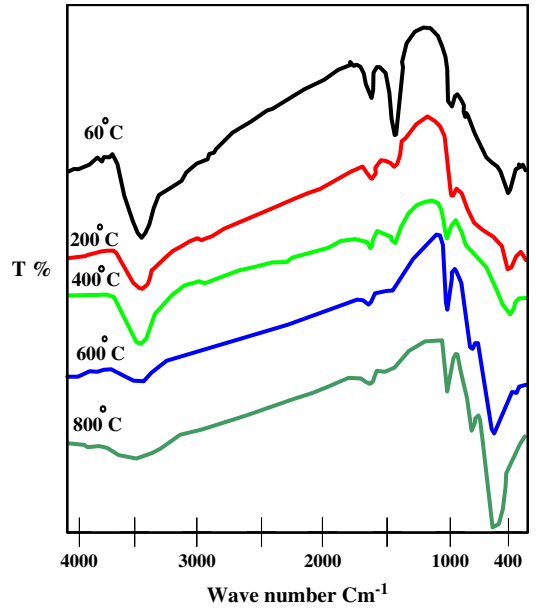

Fig. 3. IR spectra of LTVI at different drying temperature.

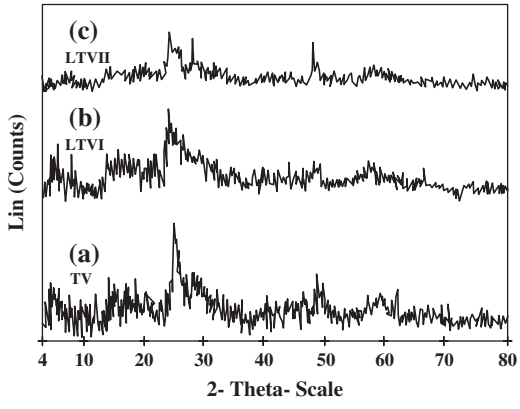

Fig. 4. X-ray diffrection pattern of (a) TV, (b) LTVI, and (c) LTVII.

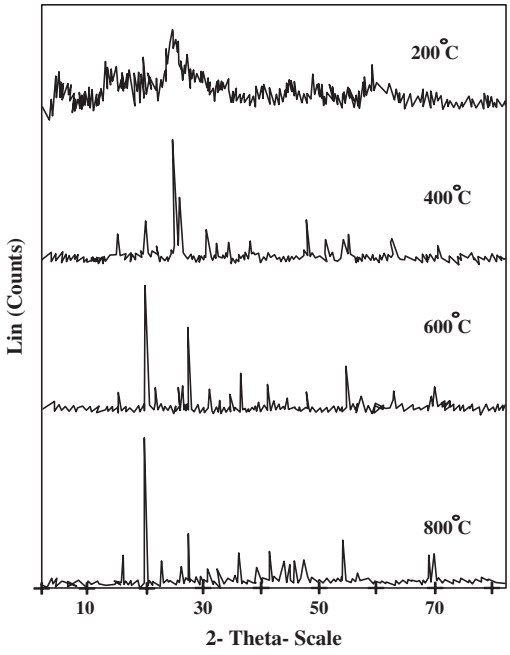

Fig. 5 X-ray diffrection pattern of LTVI at different drying temperature.

$$D = \frac{k\lambda}{\beta.\cos\theta} \quad (3)$$

where k is constant (shape factor about 0.9), λ is the X-ray wavelength (0.15406 nm), β is the full width at half maximum (FWHM) of the more intensity diffraction peak (strongest peak) (peak marker of the compound), and θ is the diffraction angle calculated from Bragg equation [30].

$$d = \frac{\lambda}{2\sin\theta} \quad (4)$$

where d is the spaces between every two diffracting planes. Data indicated that the d values are ranged in 3.5–4.5 Å (Table 4).

Morphological characterization of TV, LTVI, and LTVII exchangers was investigated using SEM (Fig. 6). It can be seen that all the prepared materials have irregular rock shapes while LTVI (Fig. 6(b)) have more defenit shape than the other two forms. Investigating the image of LTVI at different drying temprature (Fig. 7) indicated that the morphology of the surface was changed by heating, which is confident with XRD results. Some fissures appear on the surface of the particles and the size is reduced to about half by heating at 200°C, at 600°C the shape of the particles changed to needle shape with size equal 64.6 nm (Table 4). According to these results appear that, LTVI suffer crystalline as well as particle size changes against temperature.

3.2. Distribution studies

To study the effect of pH on the sorption of Sr^{2+}, Fe^{3+}, and Al^{3+} from their aqueous solution on different vanadates, equilibration was carried out in the pH range 1–5. Fig. 8 shows a plot of log K_d against pH. It

Table 4
XRD data for LTVI at different drying tempareture

Temp.	Bragg angle (2θ)	Crystallite size, D (nm)	d value Å	% of water content
60	25.00	68.0	3.48	17
200	25.60	102.0	3.47	8.5
400	25.37	35.2	3.50	4.25
600	20.32	64.6	4.36	0
800	20.32	96.2	4.36	0

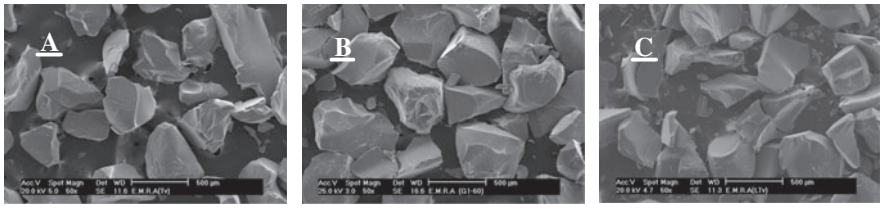

Fig. 6. Scanning electron microscope image of (A) TV, (B) LTVI, and (C) LTVII.

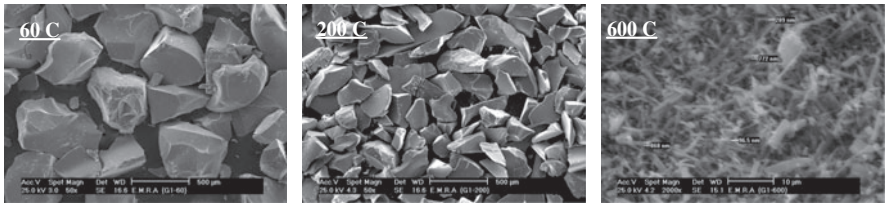

Fig. 7. Scanning electron microscope image of LTVI dried at 60, 200, and 600°C.

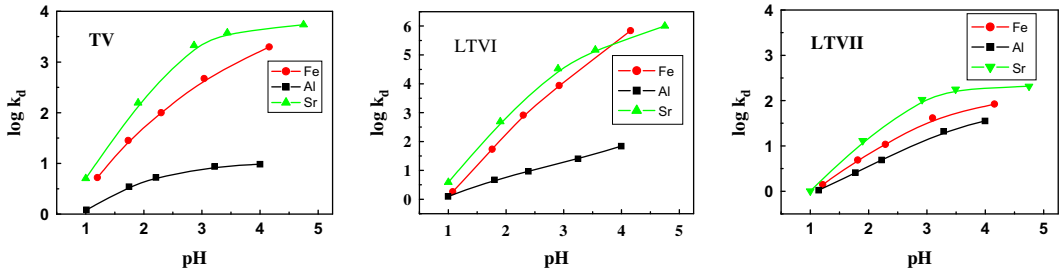

Fig. 8. log K_d of Sr^{2+}, Fe^{3+}, and Al^{3+} ions as a function of pH on TV, LTVI, and LTVII.

is noted that the ions are adsorbed mainly at higher pH values. Whereas the removal percent was zero at pH 1 it attained a maximum at pH 5 which is a common behavior [31]. The data of equlibrium were reported in Table 5. The low sorption at low pH value may be due to the competition of H_3O^+ with metal ions toward the sorption sites [32,33] According Fig. 8, niether straight line nor the slope equal the valence of the studied ions was obtained, which prove the non-ideality of the exchange reaction. These findings cannot be explained only in terms of electrostatic interaction between the hydrated cations and the anionic sites in the exchanger. It may be considered that the dependence of K_d of cations cannot be understood by a purely columbic interaction, but also may be by the formation of a covalent bond similar to a weakly acidic resin [28]. It was found that the selectivity order of the investigated cations on TV, LTVI, and LTVII reveales the sequence; $Sr^{2+} > Fe^{3+} > Al^{3+}$. Sr^{+2} revealed the highest ion selectivity compared to the other ions because of its low hydration energy, since the hydration energies of Sr^{2+}, Fe^{3+}, and Al^{3+} are −1,443, −4,430, and −4,665 kJ/mol, respectively. The gap in slectivity sequence was found to increase at high pH values which enable to resonable separation. According to data in Table 5, it is clear that separation factors between Sr^{2+} and the other ions are very large in case of LTVI, which is in agreement with the data reported by El-Naggar et al. [34]. Such separations of Sr^{2+}–Fe^{3+}, Al^{3+}–Fe^{3+}, and Sr^{2+}–Al^{3+} at pH 1.7, 2.7, 3.4, and 4.5 are indicated in Table 5. It is evident from these results that LTVI appears to be promising for ions separation from aqueous media. Regarding to the obtained values of K_d and the separation factors Table 5 the high specificity for strontium represent a unique feature of titanium vanadate and in this aspect it stands out from other titanium-based exchangers. The same result was reported earlier [35]. Furthermore, Table 6 shows the distribution coefficient values of Sr^{2+}, Fe^{3+}, and Al^{3+} on LTVI as compared to the other ion exchange materials. According to the results obtained, it can be intense, the effort in this work with the LTVI

Table 5
K_d values (ml/g) and separation factors (α) of Sr^{2+}, Fe^{3+}, and Al^{3+} as a function of pH on LTVI at 25°C and at mesh size 318 μm

	K_d values and separation factors (α)		
pH	Al^{3+}	Fe^{3+}	Sr^{2+}
1.7	4.71	53.95 (11.45)	487.5 (9.04) (103.5)
2.7	9.25	288.4 (31.18)	33,189 (115) (3,588)
3.4	25.11	8,511 (338.96)	148,696 (14.5) (5,945)
4.5	69.18	9,885.5 (10,000)	999,907 (1.44) (14,453)

Table 6
Comparison of K_d values (ml/g) of Sr^{2+}, Fe^{3+}, and Al^{3+} on various inorganic ion exchangers at 25°C and at neutral pH

Inorganic ion exchanger	Sr^{2+}	Fe^{3+}	Al^{3+}	Reference
Titanium vanadate	20,400	–	–	[35]
Magnesium silicate	–	162.1	–	[31]
Zr(IV) tungstomolybdate	328	1,368	3,218	[9]
Zr(IV) selenomolybdate	2,650	800	525	[10]
Titanium (IV) molybdophosphate				
$TiCl_4$: Molypdophosphoric acid				
1:1	6,300	–	–	
1:2	2,500			
1:3	161			
Tin vanadate	–	60.15	–	[19]
Titanium potassium vanadate	–	109.64	–	[19]
LTVI	999,907	9885.5	69.18	This work

as a promised and high efficiency for ions removal and Sr^{2+} separation.

In terms of sorption capacity Table 7, it was found that the capacity of LTVI dried at 60°C for Sr^{2+} was 1.16 meq/g, for Fe^{3+} was 0.95 meq/g and for Al^{3+} was 0.73 meq/g. However, when the sample was dried to high temperature, the sorption capacity for the studied metal ions was decreased gradually with increasing the drying temperature from 60 to 800°C. It is obvoius that, LTVI retained about 34.0% of the initial capacity at 200°C followed by deacrease by the increase in temperature. This change may be concerned with the loss of free water as well as the hydroxide groups (i.e. a negligible Li^+ substitution and H^+ deficiency), which may act as exchangeable active sites [31,36]. In addition, when the temperature was increased higher (up to 800°C) the XRD patterns of the material showed sharp improvement in crystallinity. This result deduced that an inverse relationship between the crystallinty and sorption capacity. Chen et al. [37] reported that the change away from the amorphous structure of a Fe–Ti oxide nano-adsorbent at high calcination temperature caused a decreased sorption capacity for fluoride.

3.3. Mechainsm of ion exchange process

At a solid–liquid interface, the ions uptake may take place via different mechanisms such as ion exchange, chemical reaction, and/or adsorption processes [38]. An experiment to decide what is the virtually sites that are responsible about sorption process was performed. Equlibrition of LTVI sample with 0.05 M Sr^{2+} solution (pH 5.1) for 6 h (equlibrium time) was carried out. The equlibrium pH and the released ions concentration was detected. Based on this result, it was observed that pH of solution was decreased from 5.1 to 3.1 and the Li^+ in the solution (after equilibrium) was found to be 9 ppm. Thus, mixed ion exchange process is the proposed mechanism, where as both H^+ of LTVI(OH) and the Li^+-doped in LTVI interlayers were replaced with Sr^{2+}. Such result confirms and interprets why LiTVI has high sorption capacity compared with the undoped one (TV). Ali [39] reported that, rare earth-doped sodium titanate revealed more than one active exhange site after dopining. On the other hand, by investigating the morphology of the LTVI and LTVI loaded with strontium ions, it is clear that Sr^{2+} make some agglomerations on the surface (Fig. 9). This result confirms that the uptake of Sr^{2+} may be at least on the surface of LTVI. At the same time, this surface agglomerations may be attributed to the electrostatic interaction of Sr^{2+}-LTVI [40].

The following reactions may represent the proposed processes during moving of metal ions (Sr^{2+}) from solution to the surface then through the pores and lattice channels of LTVI.

Table 7
Effect of drying temperature on sorption capacity (meq/g) of Sr^{2+}, Fe^{3+}, and Al^{3+} on LTVI

Drying Temp.	Al^{3+}	Fe^{3+}	Sr^{2+}	% loss of capacity for Sr^{2+}
60	0.73	0.95	1.16	–
200	0.20	0.29	0.40	66.15
400	0.13	0.16	0.21	82.34
600	0.10	0.12	0.18	84.27

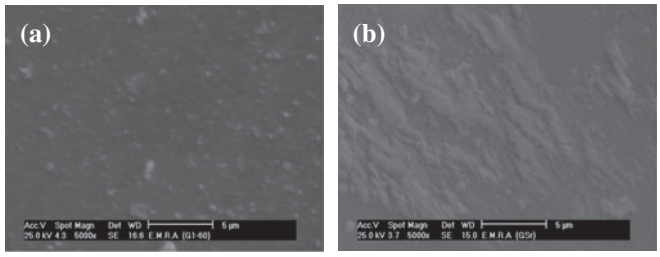

Fig. 9. Scanning electron microscope image of (a) LTVI and (b) LTVI-loaded with Sr^{2+}.

In the case of exchange with lithium ions,

$$2-\mathrm{Li}_{(\mathrm{LTVI})}+\mathrm{Sr}^{2+}_{(\mathrm{solution})}\rightarrow -\mathrm{Sr}_{(\mathrm{LTVI})}+2\mathrm{Li}^{+}_{(\mathrm{solution})}$$

When the exchange site is a hydroxyl group,

$$2-\mathrm{O}-\mathrm{H}_{(\mathrm{LTVI})}+\mathrm{Sr}^{2+}_{(\mathrm{solution})}\rightarrow (-\mathrm{O}-)_2\mathrm{Sr}_{(\mathrm{LTVI})}+2\mathrm{H}^{+}_{(\mathrm{solution})}$$

It seems that once Sr(II) ions are adsorbed and have penetrated into the interlayer region and they become immobile [41,42].

3.4. Thermodynamic studies

In any adsorption procedure, both energy and entropy considerations should be taken into account in order to determine which process will take place spontaneously. The values of the thermodynamic parameters are the actual indicators for the practical application of a process. The effect of temperature on the studied cation uptake of the adsorbents was studied. As shown in Table 8 it was found that the K_d values of Sr^{2+}, Fe^{3+}, and Al^{3+} on TV, LTVI, and LTVII were increased with increase in temperature from 298 to 338°K (i.e. the K_d value was decreased with increasing $1/T$). This trend can be attributed to acceleration of some originally slow adsorption steps and creation of some new active sites on the adsorbent surfaces [36,43–45].

The standard energy change (ΔG°), standard enthalpy change (ΔH°), and the standard entropy change (ΔS°) were calculate from the temperature-dependent equlibrium distribution as following:

$$\Delta G^\circ = -RT\ln K_d \tag{5}$$

$$\ln K_d = -\frac{\Delta G^\circ}{RT} \tag{6}$$

$$\Delta G^\circ = \Delta H^\circ - \mathrm{T}\Delta S^\circ \tag{7}$$

$$\ln K_d = -\frac{(\Delta H^\circ - T\Delta S^\circ)}{RT} = \frac{-\Delta H^\circ}{RT} + \frac{\Delta S^\circ}{R} \tag{8}$$

Table 8
Thermodynamic parameters for exchange of Sr^{2+}, Fe^{3+}, and Al^{3+} on TV at 100 ppm, 25°C, neutral pH, and at 318 μm mesh size

Metal ion	Temp. (K)	ΔG° (kJ mol^{-1})	ΔH° (kJ mol^{-1})	ΔS° (J mol^{-1} K^{-1})
Sr^{2+}	298	−21.32	16.16	125.8
	313	−23.45		126.5
	333	−25.73		125.8
Fe^{3+}	298	−17.43	56.42	247.82
	313	−21.67		249.48
	333	−26.13		247.91
Al^{3+}	298	−5.617	37.65	145.20
	313	−7.72		144.97
	333	−10.69		145.19

$$\log K_d = -\frac{\Delta H^\circ}{2.303RT} + \frac{\Delta S^\circ}{2.303R} \quad (9)$$

where R is the general gas constant = 8.314 J/mol. K and T is the absolute temperature. Plotting $\log K_d$ against $1/T$ for Sr^{2+}, Fe^{3+}, and Al^{3+} sorption at neutral pH (Fig. 10), give a straight lines with slope equal $-\Delta H^\circ/2.303R$ and an intercept equal $\Delta S^\circ/2.303R$. From the slopes and intercepts of the straight lines represented in Fig. 10, both ΔH° and ΔS° were evaluated and summarized in Table 8. The obtained positive values of ΔH° indicate the endothermic nature of the adsorption process [46], while the positive values of ΔS° indicate the increased randomness at solid–solution interface during the sorption of the cations. Evaluation of thermodynamic parameters provide an insight into mechanism of Sr^{2+}, Fe^{3+}, and Al^{3+} sorption in each vanadates. The negative values of the free energy change (ΔG°), for the investigated ions indicate that the adsorption process is spontaneous and also reveal a preferable sorption of the studied cations on LTVI as compared to H^+. It was found that the negativity of ΔG° increases in the order, $Sr^{2+} < Fe^{3+} < Al^{3+}$ which agrees with the selectivity sequence of the material for these cations as well as increasing. Furthermore, it was found that ΔG° increases as the temperature increases which indicating that the cations sorption is more favoured at higher temperature. Similar results were reported for sorption of Zn^{2+} on some calcareous soils [47].

3.5. Adsorption isotherms

The adsorption isotherm indicates the distribution relationship of the adsorbate molecules between the liquid phase and the solid phase when the adsorption process reaches equilibrium. The results obtained for Sr^{2+}, Fe^{3+}, and Al^{3+} sorption on LTVI were analyzed with well-known adsorption models, Langmuir and Freundlich.

3.5.1. Langmuir model

The Langmuir isotherm is a commonly applied model for adsorption on a completely homogenous surface with negligible interaction between adsorbed molecules [48]. The model assumes uniform adsorption energies onto the surface and maximum adsorption depends on saturation level of monolayer. Langmuir model can be represented with the following linear equation:

$$\frac{C_e}{q_e} = \frac{C_e}{Q} + \frac{1}{bQ} \quad (10)$$

where q_e represents the mass of adsorbed ions per unit sorbent (mg/g), Q is the monolayer capacity, b is the equilibrium constant, and C_e is the equilibrium concentration of the solution (mg/L). Plot of C_e/q_e vs. q_e (Fig. 11) should indicate a straight line of slope $1/Q$ and an intercept of $1/bQ$, which demenostrate that the sorption system well obyed to this model. The applicability of this model gives predication that the main mechanism for Sr^{2+}, Fe^{3+}, and Al^{3+}ions separation using the synthesized material may take place through the ion exchange process as monolayer at the ion exchange material [27]. The Langmuir parameters for Sr^{2+}, Fe^{3+}, and Al^{3+} removal (Q and b) were calcated and tabulated in Table 9. The maximum monolayer sorption capacity of Sr^{2+}, Fe^{3+}, and Al^{3+}

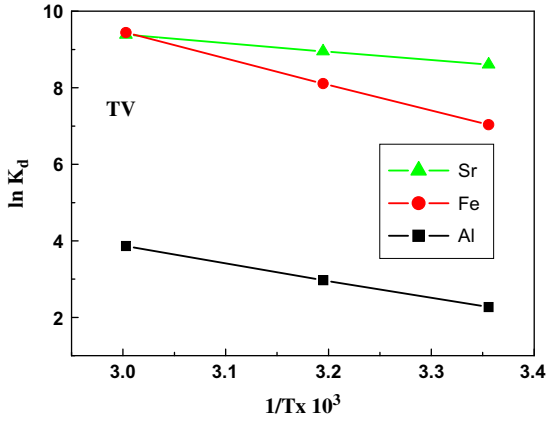

Fig. 10. Van't Hoff plot for the adsorption of Sr^{2+}, Fe^{3+}, and Al^{3+} on TV, LTVI, and LTVII at neutral pH.

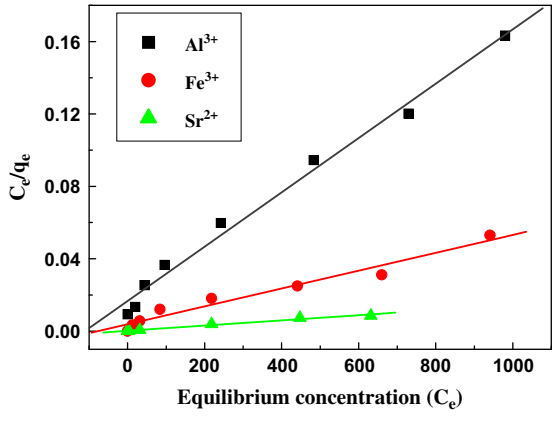

Fig. 11. Langmiur adsorption isotherm for adsorption of Sr^{2+}, Fe^{3+}, and Al^{3+} on LTVI.

Table 9
Langmuir and Frendlich isotherm parameters for Sr^{2+}, Fe^{3+}, and Al^{3+} on LTVI at 25°C, 318 μm and at neutral pH

	Langmuir isotherm			Freundlich isotherm		
	Q monolayer capacity (mol/g)	$b \times 10^{-3}$ (l/mol)	R^2	K_f (mol/g)	n	R^2
Al^{3+}	0.24	0.17	0.99	0.042	2.5	0.99
Fe^{3+}	0.40	0.79	0.98	0.050	2.4	0.98
Sr^{2+}	0.89	40.26	0.99	0.095	2.9	0.98

onto LTVI were equal to 0.89, 0.4, and 0.24 mg/g, respectively. So, the prepared cation exchanger is distinguished by high sorption capacity for the studied ions. Accordingly, it is suitable to be utilized for industrial waste water treatment processes "polluted water."

3.5.2. Freundlich model

The Freundlich model is known as the earliest empirical equation and is shown to be consistent with exponential distribution of active centers, characteristic of heterogeneous surfaces [48,49]. Freundlich equation is:

$$\log q_e = \log k_f + \frac{1}{n} \log C_e \quad (11)$$

where k_f and n represent adsorption capacity and intensity, respectively. k_f is an important constant used as relative measure for adsorption efficiency. The magnitude of the n shows an indication of the favourability of adsorption. Values of n larger than one show the favorable nature of adsorption [50,51]. The plot of $\log C_e$ against $\log q_e$ for Sr^{2+}, Fe^{3+}, and Al^{3+} sorption data on the prepared cation exchanger is fitting well to the Freundlich isotherm (Fig. 12). Accordingly, it can be seen that the adsorption isotherms of Sr^{2+}, Fe^{3+}, and Al^{3+} on LTVI are fitted well by both Langmuir and Freundlich models [27]. The n value that is more than one, Table 9, confirms the favourability nature of Sr^{2+}, Fe^{3+}, and Al^{3+} sorption onto the prepared materials [52]. This gives prediction that the adsorption phenomena have some degree of contribution besides the ion exchange mechanism for Sr^{2+}, Fe^{3+}, and Al^{3+} removal.

Such result is in agreement with data reported in Section 3.3. in this work which concluded that mixed mechanism took place.

The higher values of the correlation coefficient (R^2) for both the models suggests that the experimental data exhibit a very good mathematical fit to both the models and this can be interpreted in terms of surface

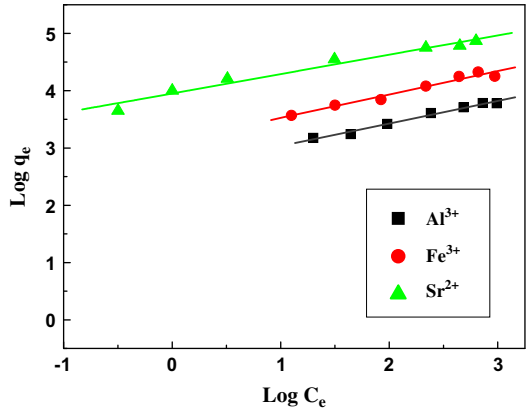

Fig. 12. Freundlich adsorption isotherm for adsorption of Sr^{2+}, Fe^{3+}, and Al^{3+} on LTVI.

nature of the adsorbent and its affinity towards studied ions. While both the models fit well, the R^2 value for Langmuir model 0.99 in case of Sr^{2+} is marginally higher than that of the Freundlich model 0.98, which may indicate the predominance of monolayer adsorption process over intramolecular interactions among the adsorbed cations [53]. In addition, similar result was reported in case of adsorption of lead on nanozirconium tungestovanadate [27].

4. Conclusions

This paper demonstrates the synthesis and characterization of titanium vanadate and its modified forms using a single-step precipitation process. All obtained vanadates showed high selectivity for Sr^{2+} compared to Fe^{3+} and Al^{3+}. LTVI that obtained using ammonia solution as precipitating agent in presence of LiCl as a source for Li ions revealed higher sorption and mechanical characters compared to the other prepared forms (TV and LTVII). Sorption process was found to be take place through two different positions (localized lithium ions and protons of hydroxide groups) on LTVI. Thermodynamic studies revealed that all sorption processes were spontaneous and endothermic

in nature. This suggests that the sorption capacity of these materials favored at high reaction temperature. The positive value of ΔS° revealed an increase in randomness of the solid–solution interface during the sorption of cations. Sorption isotherm studies indicated that the sorption process obeyed both Freundlich and Langmuir models. Finally, it can be proposed that the insertion of Li^{+} ions into vanadate matrix produced an effective material more applicable for removal of heavy metal ions from aqueous solutions.

References

[1] I.M. El-Naggar, E.S. Zakaria, I.M. Ali, M. Khalil, M.F. El-Shahat, Kinetic modeling analysis for the removal of cesium ions from aqueous solutions using polyaniline titanotungstate, Arabian J. Chem. 5 (2012) 109–119.

[2] I.M. Ali, E.S. Zakaria, M.M. Ibrahim, I.M. El-Naggar, Synthesis, structure, dehydration transformations and ion exchange characteristics of iron-silicate with various Si and Fe contents as mixed oxides, Polyhedron 27(1) (2008) 429–439.

[3] I.M. El-Naggar, E.S. Zakaria, S.A. Shady, H.F. Aly, Diffusion mechanism and ion exchange equilibria of some heavy metal ions on cerium(IV) antimonate as cation exchanger, Solid State Ionics 122(1–4) (1999) 65–70.

[4] E.S. Zakaria, I.M. Ali, I.M. El-Naggar, Thermodynamics and ion exchange equilibria of Gd^{3+}, Eu^{3+} and Ce^{3+} ions on H^{+} form of titanium(IV) antimonate, Colloids Surf., A 210(1) (2002) 33–40.

[5] N.H. Shaidan, U. Eldemerdash, S. Awad, Removal of Ni(II) ions from aqueous solutions using fixed-bed ion exchange column technique, J. Taiwan Inst. Chem. Eng. 43(1) (2012) 40–45.

[6] M.N.A. Al-Jibouri, T.M. Musa, M. Mubarak, W.M. Al-Jibouri, Synthesis characterization and adsorption study of new resin PVC8-hydroxyquinoline -5-sulfonic acid with toxic metals, Sci. J. Chem. 1(4) (2013) 38–49, doi: 10.11648/j.sjc.20130104.11.

[7] G. Mahajan, D. Sud, Accessing the potential of lingocellulosic agricultural waste biomass for removal of Ni (II) metal ions from aqueous streams, Int. J. Sci. Eng. Res. 4(4) (2013) 1713–1720. ISSN 2229-5518.

[8] V.K. Gupta, P. Singh, N. Rahman, Adsorption behavior of Hg(II), Pb(II), and Cd(II) from aqueous solution on Duolite C-433: A synthetic resin, J. Colloid Interface Sci. 275(2) (2004) 398–402.

[9] S.A. Nabi, M. Naushad, Inamuddin, Synthesis and characterization of a new inorganic cation-exchanger—Zr(IV) tungstomolybdate: Analytical applications for metal content determination in real sample and synthetic mixture, J. Hazard. Mater. 142 (2007) 404–411.

[10] A.P. Gupta, G.L. Verma, S. Ikram, Studies on a new heteropolyacid-based inorganic ion exchanger; zirconium(IV) selenomolybdate, React. Funct. Polym. 43(1–2) (2000) 33–41.

[11] V.K. Gupta, P. Singh, N. Rahman, Synthesis, characterization, and analytical application of zirconium(IV) selenoiodate, a new cation exchanger, Anal. Bioanal. Chem. 381 (2005) 471–476.

[12] P. Sharma, N. Neetu, Synthesis, characterization and sorption behavior of zirconium(IV) antimonotungstate: An inorganic ion exchanger, Desalination 267(2–3) (2011) 277–285.

[13] R.R. Sheha, S.H. El-Khouly, Adsorption and diffusion of cesium ions in zirconium(IV) iodomolybdate exchanger, Chem. Eng. Res. Des. 91 (2013) 942–954.

[14] I.M. El-Naggar, E.S. Zakaria, W.M. El-Kenawy, M.F. El-Shahat, Synthesis and equilibrium studies of titanium vanadate and its use in the removal of some hazardous elements, Radiochemistry 56(1) (2014) 77–81.

[15] X. Guo-Ping, T. Ke-Feng, S. Shu-Ying, Y. Jian-Guo, Preparation of spherical PVC-MnO_2 Ion sieve and its lithium adsorption property, Chinese J. Inorg. Chem. 28(11) (2012) 2385–2394.

[16] X. Shi, Z. Zhang, D. Zhou, L. Zhang, B. Chen, L. Yu, Synthesis of Li^{+} adsorbent (H_2TiO_3) and its adsorption properties, Trans. Nonferr. Metal Soc. China 23 (2013) 253–259.

[17] I.M. El-Naggar, M.Y. Mahmoud, E.A. Abdel-galil, inorganic ion exchange materials based on titanate: Synthesis, characterization and sorption behavior of zirconium titanate for some hazardous metal ions from aqueous waste solution, Isot. Radiat. Res. 44(4) (2012) 851–871.

[18] I.M. Ali, E.S. Zakaria, S.A. Shama, I.M. El-Naggar, Synthesis, properties and effect of ionizing radiation on sorption behavior of iron silico-antimonate, J. Radioanal. Nucl. Chem. 285 (2010) 239–245.

[19] A.B. El-Deeb, Chemical studies on the synthesis and characterization of some ion-exchange materials and its use in the treatment of hazardous wastes, PhD. Thesis, Chem. Department, Faculty of Science, Benha University, Benha, Egypt, 2013, p. 293.

[20] M. Mohapatra, L. Mohapatra, P. Singh, S. Anand, B.K. Mishra, A comparative study on Pb(II), Cd(II), Cu(II), Co(II) adsorption from single and binary aqueous solutions on additive assisted nano-structured goethite, Int. J. Eng. Sci. Res. Technol. 2(8) (2010) 89–103.

[21] M.M. Abd El-Latif, M.F. Elkady, Synthesis, characterization and evaluation of nano-zirconium vanadate ion exchanger by using three different preparation techniques, Mater. Res. Bull. 46 (2011) 105–115.

[22] Z. Chang, Z. Chen, F. Wu, X.Z. Yuan, H. Wang, The synthesis of $Li(Ni_{1/3}Co_{1/3}Mn_{1/3})O_2$ using eutectic mixed lithium salt $LiNO_3$–LiOH, Electrochim. Acta 54 (2009) 6529–6535.

[23] M.M. Abo El-Fadl, A.M. El-Aassar, A.A. Mohamed, Synthesis of nanocomposite membranes and their application in photocatalytic process for organic pollutions removal from groundwater, East Nile Delta, Egypt, in: Conference on Desalination for the Environment: Clean Water and Energy, 11–15 May 2014, Limassol, Cyprus, Desalin. Water Treat. (2014) 1–11 doi: 10.1080/19443994.2014.940218.

[24] R. Yavari, S. Ahmadi, Y. Huang, A. Khanchi, G. Bagheri, J. He, Synthesis, characterization and analytical application of a new inorganic cation exchanger-Titanium(IV) molybdophosphate, Talanta 77 (2009) 1179–1184.

[25] M. Vijayakumar, S. Selvasekarapandian, R. Kesavamoorthy, K. Nakamura, T. Kanashiro, Vibrational

and impedance spectroscopic studies on lithium vanadate prepared by solid-state reaction, Mater. Lett. 57 (2003) 3618–3622.
[26] I.M. El-Naggar, E.A. Mowafy, G.M. Ibrahim, H.F. Aly, Sorption behavior of molybdenum on different antimonates ion exchangers, Adsorption 9(4) (2003) 331–336.
[27] M.F. Elkady, E.M. El-Sayed, H.A. Farag, A.A. Zaatout, Assessment of novel synthetized nanozirconium tungstovanadate as cation exchanger for lead ion decontamination, J. Nanomater. ID 149312 (2014) 1–11.
[28] W.M. El-Kenawy, Synthesis and characterization of titanium vanadate and vanadium antimonite and their use in treatment of some toxic waste, PhD. Thesis, Chem. Department, Faculty of Science, Ain Shams University, Cairo, 2013, p. 218.
[29] M.V. Sivaiah, K.A. Venkatesan, R.M. Krishna, P. Sasidhar, G.S. Murthy, Characterization of uranium antimonite ion exchanger, Colloids Surf., A 295(1–3) (2007) 1–6.
[30] M. Khayet, M.C. García-Payo, X-Ray diffraction study of polyethersulfone polymer, flat-sheet and hollow fibers prepared from the same under different gas-gaps, Desalination 245 (2009) 494–500.
[31] I.M. Ali, Y.H. Kotp, I.M. El-Naggar, Thermal stability, structural modifications and ion exchange properties of magnesium silicate, Desalination 259 (2010) 228–234.
[32] V. Tharanitharan, R. Kalaivani, Adsorption of heavy metal ions from water and wastewater using modified acrylic ester polymeric resin, Chem. Sci. Rev. Lett. 2(5) (2014) 393–401.
[33] A.M. Ziyath, P. Mahbub, A. Goonetilleke, M.O. Adebajo, S. Kokot, A. Oloyede, Influence of physical and chemical parameters on the treatment of heavy metals in polluted stormwater using zeolite—A review, J. Water Resour. Prot. 3 (2011) 758–767.
[34] I.M. El-Naggar, E.A. Mowafy, E.A. Abdel-Galil, M.F. El-Shahat, Synthesis, characterization and ion-exchange properties of a novel 'organic-inorganic' hybrid cation-exchanger: polyacrylamide Sn(IV) molybdophosphate, Global J. Phys. Chem., V. 1(1) (2010) 91–106.
[35] M.M. Qureshi, K.G. Varshney, S. Kabiruddin, Synthesis and ion exchange properties of thermally stable titanium(IV) vanadate: separation of Sr^{2+} from Ca^{2+}, Ba^{2+}, and Mg^{2+}, Can. J. Chem. 50 (1972) 2071–2078.
[36] E.A. Abdel-Galil, Chemical studies and sorption behavior of some hazardous metal ions on polyacrylamide stannic molybdophosphate as organic-inorganic composite cation-exchanger, PhD. Thesis, Chem. Department, Faculty of Science, Ain Shams University, Cairo, 2010, p. 304.
[37] L. Chen, B. He, S. He, T. Wang, C. Su, Y. Jin, Fe—Ti oxide nano-adsorbent synthesized by co-precipitation for fluoride removal from drinking water and its adsorption mechanism, Powder Technol. 227 (2012) 3–8.
[38] E. Erdem, N. Karapinar, R. Donat, The removal of heavy metal cations by natural zeolites, J. Colloid Interface Sci. 280 (2004) 309–314.
[39] I.M. Ali, Synthesis and sorption properties of new synthesized rare-earth-doped sodium titanate, J. Radioanal. Nucl. Chem. 285 (2010) 263–270.
[40] J.M. Mathes, Protein adsorption to vial surfaces—Quantification, structural and mechanistic studies, PhD.Thesis, Faculty of Chemistry and Pharmacy, University of Munich, (2010).
[41] K.M. Elsabawy, M.M.A. Sekkina, A.T. Tawfik, green synthesis of nano-fe–biotite for removal of hazardous metals ions from aqueous solutions, Eur. Chem. Bull 1 (7) (2012) 250–257.
[42] S.Y. Lee, M.H. Baik, Y. Lee, Adsorption of U(VI) ions on biotite from aqueous solutions, J. Appl. Clay Sci. 46(3) (2009) 255–259.
[43] S.E. Ghazy, A.H.M. Gad, Lead separation by sorption onto powdered marble waste, Arabian J. Chem. 7 (2014) 277–286.
[44] M.C. Menkiti, M.C. Aneke, P.M. Ejikeme, O.D. Onukwuli, N.U. Menkiti, Adsorptive treatment of brewery effluent using activated *Chrysophyllum albidium* seed shell carbon, Springer Plus 3 (2014) 213. http://www.springerplus.com/content/3/1/213.
[45] U. Nadeem, Adsorptive removal of Pb(II) and Cr(VI) ions on natrolite, Eur. Chem. Bull. 3(5) (2014) 495–501.
[46] I.M. Ali, Sorption studies of ^{134}Cs, ^{60}Co and $^{152+154}Eu$ on phosphoric acid activated silico-antimonate crystals in high acidic media, Chem. Eng. J. 155 (2009) 580–585.
[47] S.D. Nystrom, Thermodynamic parameters of zinc sorption in some calcareous soils, Int. J. Agric. Environ. 1 (2012) 1–7.
[48] F. Gode, E. Pehlivan, Adsorption of Cr(III) ions by Turkish brown coals, Fuel Process. Technol. 86(8) (2005) 875–884.
[49] R. Naseem, S.S. Tahir, Removal of Pb(II) from aqueous/acidic solutions by using bentonite as an adsorbent, Water Res. IWA 35(16) (2001) 3982–3986.
[50] Y.S. Ho, Effect of pH on lead removal from water using tree fern as the sorbent, Bioresour. Technol. 96 (11) (2005) 1292–1296.
[51] E. Veliev, T. Ozt¨urk, S. Veli, A. Fatullayev, Application of diffusion model for adsorption of azo reactive dye on pumice, Pol. J. Environ. Stud. 15(2) (2006) 347–353.
[52] I.M. El-Naggar, E.S. Zakaria, I.M. Ali, M. Khalil, M.F. El-Shahat, Removal of cesium on polyaniline titanotungstate as composite ion exchanger, Adv. Chem. Eng. Sci. 2 (2012) 166–179.
[53] P.R. Rout, P. Bhunia, R.R. Dash, Modeling isotherms, kinetics and understanding the mechanism of phosphate adsorption onto a solid waste: Ground burnt patties, J. Environ. Chem. Eng. 2 (2014) 1331–1342.